POLITECNICO DI TORINO
Repository ISTITUZIONALE

Waveband selective switch: a networking analysis for advanced optical transport networks in 6G and beyond technologies

(Article begins on next page)

04 May 2024

Waveband Selective Switch: A Network Analysis for Advanced Optical Transport Networks in 6G and Beyond Technologies

Muhammad Umar Masood[a], Ihtesham Khan[a], Lorenzo Tunesi[a], Bruno Correia[a], Andrea Marchisio[a], Enrico Ghillino[b], Paolo Bardella[a], Andrea Carena[a], and Vittorio Curri[a]

[a]DET, Politecnico di Torino, Corso Duca degli Abruzzi 24, Torino, Italy
[b]Synopsys, Inc., 400 Executive Blvd Ste 101, Ossining, NY 10562, United States

ABSTRACT

Multi-layer optical networks are a prospective concept in the upcoming era of bandwidth-abundant optical networks that decouple the enormous spatial division multiplexing (SDM) layer from the wavelength division multiplexing layer. In this direction, we present an analysis of a generalized multi-band optical cross-connect (OXC) at the networking level. This OXC operates in two stages: firstly, it groups wavelengths to form wavebands, and secondly, it switches them as waveband paths. The findings demonstrate that waveband routing is a viable and cost-effective replacement for traditional wavelength routing in massive parallel optical networks.

Keywords: Multi-layer optical networks; Waveband Switching; Multi-band optical networks.

1. INTRODUCTION

Recent technological advancements, including 5G and the upcoming 6G mobile communication, cloud computing, and high-bandwidth applications like video-oriented services, contribute to the exponential growth of Internet traffic.[1] This exponential increase in traffic necessitates bandwidth-rich, cost-effective optical networks to serve enormous data capacities. Important in this regard is the creation of large-scale OXC.[2] Currently, many working optical switching systems, such as reconfigurable optical add-drop multiplexers (ROADM) and OXC, are made with wavelength-selective switches (WSSs), which can hold up to 35 ports.[3] The cascading of numerous WSSs is the principal approach to achieving the port count requirement and generating OXCs of significant magnitude. In large-scale OXCs, the quantity of cascaded WSSs is nearly equal to the square root of the degree.[2] Additionally, it should be noted that cascaded WSS progressively incurs a more significant transmission loss at each stage. Consequently, additional amplifiers are required to counterbalance this loss, which adds noise to the system. As optical transmission systems increasingly transition to multi-band and multi-core configurations in the upcoming era of 6G communication, traditional wavelength (WL) switching will substantially increase cost and complexity.[4] In this regard, waveband (WB) switching is a simple and potentially inexpensive solution. All WB's grouped wavelengths are routed simultaneously when the WB groups up different WL routes. Although employing WB switching instead of traditional WL switching can simplify and lower hardware costs, there is a small performance hit from a lack of fine-grained routing. However, this can be mitigated with proper spectrum assignment and routing schemes.[5]

We analyzed the networking performance of an optical node switching system for multi-band optical networks in this research. This system implements switching in two stages: first, it groups WLs, and second, it switches those WLs as WB pathways. A collection of several continuous WLs is aggregated and forms a WB for each input port. This study considers the OXC architecture suggested in,[6] which utilizes dynamic optical filters with minimal port counts for two frequency bands (C+L) to generate WBs. In this study, we studied a single modular multi-band WSS that can operate in the low-loss zone, i.e., C+L+S bands,[7] as opposed to[6] employing separate WSSs for the (C+L) bands. The analysis conducted in this study demonstrates that classic WL routing is no longer viable for upcoming bandwidth-abundant optical networks where routing bandwidth increases and sooner or later reaches fiber or full-band routing; a simple and cost-effective replacement to traditional WL routing is WB routing.
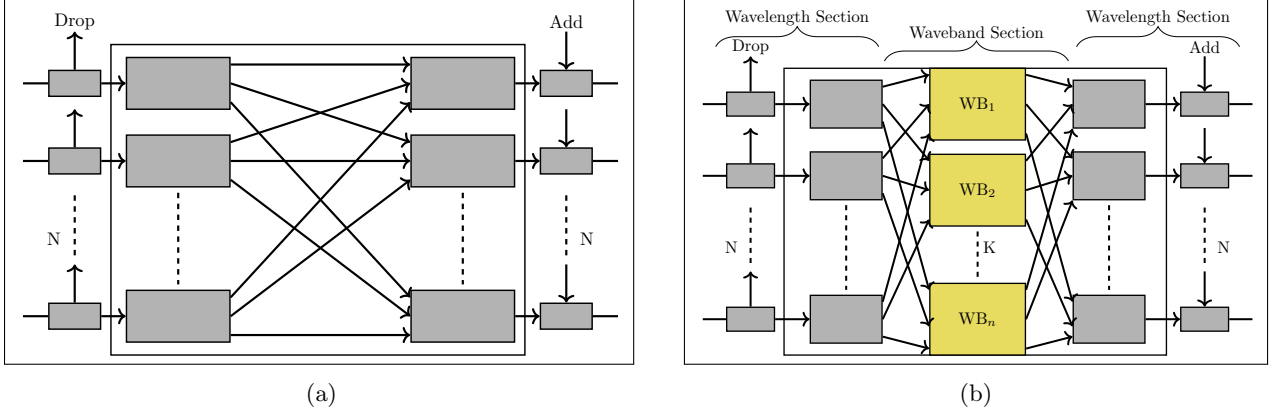
Figure 1: (a) Wavelength enabled node architecture; (b) Waveband enabled node architecture.

2. NETWORKING ANALYSIS

To study how single-layer conventional WL switching and the multi-layer WB architecture affect different optical transport configurations, the network's overall performance needs to be looked at in detail. For this objective, we employ the statistical network assessment process (SNAP).[8] SNAP focuses on the physical layer of the examined network and assesses the degradation in quality of transmission (QoT) induced by each network element. The QoT metric is the generalized signal-to-noise ratio (GSNR), which includes both P_{ASE} and P_{NLI}.

$$\text{GSNR}_{\text{i}} = \frac{P_{\text{S,i}}}{P_{\text{ASE}(f_i)} + P_{\text{NLI,i}}(f_i)} \, , \tag{1}$$

for the ith channel with centre frequency f_i, where $P_{\text{S,i}}$ is the transmitted power of the signal, $P_{\text{ASE}(f_i)}$ is the amplified spontaneous emission, and $P_{\text{NLI,i}}(f_i)$ is the non-linear interference of the fiber. The simulation was conducted for a multi-band optical system, specifically focusing on the networking components required for a multi-band transmission system, with a particular emphasis on optical amplifiers.[9] The amplifiers considered in this analysis are commercially available erbium-doped fiber amplifiers (EDFAs) designed for C- and L-bands, as well as thulium-doped fiber amplifiers (TDFAs) intended for the S-band.[10] The optical fiber used in the amplified lines is a standard single-mode fiber with a span length of 75 km.

In this work, a comprehensive investigation was undertaken for a 1.2T transmission system utilizing a transceiver with a free spectral range (FSR) of 150 GHz and a symbol rate of 130 GBaud. The optimization of input power for each band was performed through a span-by-span strategy employing the Local Optimization Global Optimization (LOGO) algorithm,[11] with a primary focus on maximizing QoT. In addition to this, two switching architectures were considered for comparison: the conventional WL switching system and the WB switching system. In the WB switching architecture, the WLs are initially grouped while adhering to continuity constraints, with consideration given to a minimum of 2 WLs per band (M = 2) and a maximum of 6 WLs per band (M = 6). These clustered WLs are then routed together as a single WB at a given time.

The analysis further takes into account the Italian network topology, comprising 21 optical nodes and 36 edges with an average node degree of 3.43. The ROADMs and OXCs are treated as optical nodes where traffic requests are added or dropped, while the edges represent the optical line systems, including fiber pairs and inline amplifiers. Lastly, a uniform traffic distribution for all nodes in the network is assumed for this simulation.

3. RESULTS AND CONCLUSION

To evaluate the influence of the WB architecture on networking performance in comparison to the conventional WL architecture, we conducted simulations encompassing various network scenarios and a uniform traffic profile.

Fig. 2a depicts the distribution of network traffic with respect to blocking probability (BP) for both the conventional WL architecture with a single wavelength ($M = 1$) and the WB architectures across a spectrum of
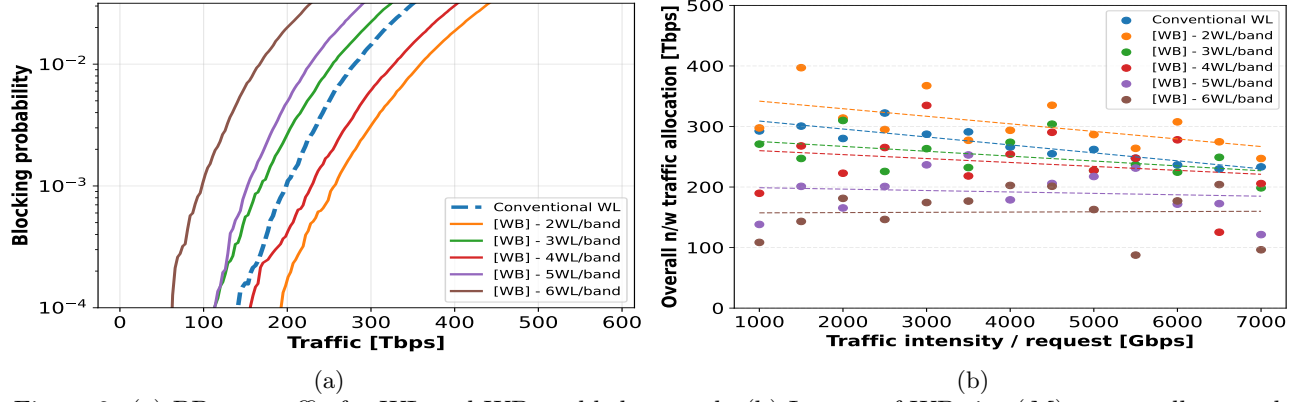
Figure 2: (a) BP vs. traffic for WL and WB enabled network; (b) Impact of WB size (M) on overall network traffic;.

values for M, specifically ranging from $M = 2$ to $M = 6$. The simulations were conducted under a consistent and fixed uniform traffic profile, with a request volume of 3000 Gbps per request. In the context of the specified traffic profile, with a fixed blocking probability ($BP = 10^{-2}$), the conventional WL configuration allocates approximately 280 Tbps. In contrast, the WB configuration with $M = 2$ allocates approximately 366 Tbps, representing a 30.7% increase. As we explore higher values of M (i.e., $M = 3, 4, 5$), the overall traffic allocation experiences variations of approximately 266 Tbps (a 5% reduction), 330 Tbps (a 17.86% increase), and 231 Tbps (a 17.5% reduction), respectively. However, when $M = 6$, the overall traffic allocation notably decreases to approximately 169 Tbps, indicating a significant reduction of 39.64% compared to the $M = 1$ case. It is noteworthy that for $M = 3, 5$, and 6, the traffic allocation is lower than that of the $M = 1$ case, attributed to spectrum wastage for the specific 3000 Gbps traffic profile.

Fig. 2b presents an overview of network performance, specifically focusing on overall traffic allocation across a spectrum of traffic intensities while maintaining a fixed blocking probability of 10^{-2}. As the traffic intensity per request rises, a reduction is observed in the overall allocation of network traffic for the WB architecture, spanning values of M from 2 to 6. A distinct comparison between the conventional WL and WB cases reveals a significant disparity: the steeper slope in the conventional WL implies an earlier onset of traffic request blocking, stemming from constraints associated with limited channel bandwidth. However, it is noteworthy that while the conventional WL exhibits a steeper slope in overall network traffic allocation, the trend indicates that, as traffic intensity further increases, the WB configurations are poised to surpass the WL case.

The increasing demand for high-intensity bandwidth to accommodate emerging technologies underscores the need for effective and robust solutions. This study has presented an evaluation of WB switching in comparison to conventional WL switching, shedding light on its impact on the overall networking landscape. The findings strongly suggest that WB switching demonstrates superior performance compared to conventional approaches, positioning it as a promising and advantageous choice to address the evolving bandwidth requirements of the future.

REFERENCES

[1] Cisco, "Annual internet report (2018–2023) white paper."

[2] Hasegawa, H., "Bandwidth abundant optical networking enabled by spatially-jointed and multi-band flexible waveband routing," *IEICE Transactions on Communications* (09 2023).

[3] Matsuo, T., , et al., "Architecture and performance evaluation of fiber-granularity routing networks with supplemental grooming by wavelength conversion," *JOCN* **15**, 541–552 (Aug 2023).

[4] Munakata, R. et al., "Architecture and performance evaluation of bundled-path-routing multi-band optical networks," in [*OFC*], 1–3, IEEE (2023).

[5] Munakata, R. et al., "Design and performance evaluation of resilient optical path networks that adopt spatially-jointed flexible waveband routing," in [*ONDM*], 1–6, IEEE (2021).

[6] Munakata, R. et al., "Architecture and performance evaluation of bundled-path-routing multi-band optical networks," in [*OFC 2023*], *Optical Fiber Communication Conference (OFC) 2023* , M4G.8, Optica Publishing Group (2023).

[7] Tunesi, L. et al., "Design and performance assessment of modular multi-band photonic-integrated WSS," *Opt. Express* **31**, 36486–36502 (Oct 2023).

[8] Cantono, M., Gaudino, R., and Curri, V., "The statistical network assessment process (SNAP) to evaluate benefits of amplifiers and transponders' upgrades," in [*18th Italian National Conference on Photonic Technologies (Fotonica 2016)*], 1–4 (2016).

[9] Ferrari, A., Napoli, A., Fischer, J. K., Costa, N., D'Amico, A., Pedro, J., Forysiak, W., Pincemin, E., Lord, A., Stavdas, A., et al., "Assessment on the achievable throughput of multi-band itu-t g. 652. d fiber transmission systems," *Journal of Lightwave Technology* **38**(16), 4279–4291 (2020).

[10] Correia, B. et al., "Power control strategies and network performance assessment for C+L+S multiband optical transport," *JOCN* **13**(7), 147–157 (2021).

[11] Curri, V., Carena, A., Arduino, A., Bosco, G., Poggiolini, P., Nespola, A., and Forghieri, F., "Design strategies and merit of system parameters for uniform uncompensated links supporting nyquist-wdm transmission," *Journal of Lightwave Technology* **33**(18), 3921–3932 (2015).